

Adaptive Active Noise Control in Free Space

Iman Tabatabaei Ardekani* and Waleed H. Abdulla†

* Computing Dept., Unitec Institute of Technology, Auckland, New Zealand

† Electrical and Computer Eng. Dept., The University of Auckland, Auckland, New Zealand

Abstract—This paper develops a reliable methodology for active control of acoustic noise in free space. The core of this paper consists of a root locus analysis on the adaptation process performed in active noise control. Based on this analysis, a novel active noise control algorithm is derived. This algorithm is fully implemented in an experimental setup. Different experiments with this setup show that the traditional active noise control algorithm is not stable when the setup is used in free space. However, the proposed algorithm is stable and converges at a high convergence rate until the noise level is reduced by 15 dB in steady-state conditions.

I. INTRODUCTION

Fig. 1 shows a general block diagram for single-channel ANC with feed-forward structure [4], [12]. $x(n)$, $y(n)$ and $e(n)$ represent reference noise, anti-noise and residual noise in the electric domain, respectively. $x(n)$ is obtained by measuring the sound pressure at a location close to the noise source. $e(n)$ is obtained by measuring the sound pressure at the desired zone of silence, Z_s . $y(n)$ is generated in the electric domain and fed to a loudspeaker. The sound generated by this loudspeaker propagates through an acoustic channel, S , to reach Z_s (secondary path). On the other hand, the noise generated by the noise source, propagates through another acoustic channel, P , to reach Z_s (primary path). These two signals combine acoustically with each other across the medium; however, $e(n)$ that is the net sound pressure at Z_s is only taken as a measure of the residual noise.

ANC algorithms adaptively minimize $e(n)$ in the acoustic domain. These algorithms perform two tasks: i) computing $y(n)$ as the response of an adaptive filter, W , to $x(n)$ and ii) updating the weight vector of W , $w(n)$, by using an update equation, e.g. the FxLMS update equation [15] given by

$$w(n+1) = w(n) + \mu e(n) s(n) \otimes x(n) \quad (1)$$

where \otimes denotes the linear convolution, μ is the step-size and $s(n)$ is the impulse response of S . ANC systems can attenuate the noise propagating in a duct by about -20dB in practice [1], [3], [7], [9]. However, they cannot significantly attenuate the noise propagating in free space. The implementation of ANC algorithms in ducts or headphones is successful because the sound propagation model in them is relatively simple. Accordingly, most of available ANC algorithms are efficient in the acoustic media similar to ducts [11], [14], [16] or headphones [5], [6], [13]. The sound propagation in free space is so complicated that requires W to be updated more intelligently in order to cope with changes in medium or noise characteristics. Otherwise, the adaptation process diverges. For surpassing this problem, one may suggest to use more sophisticated ANC algorithms, e.g. FxRLS or FxAP [14] but a

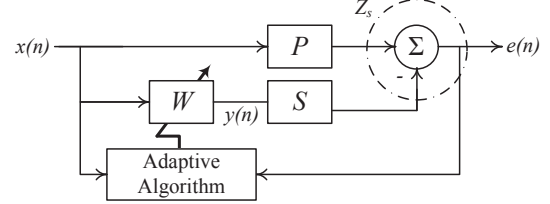


Fig. 1: Block diagram for single-channel feed-forward ANC

common drawback of these algorithms is their implementation cost. For example, we reported a successful implementation of FxLMS algorithm and some of its variants [1], [10]; however, we found that the implementation of FxRLS or FxAP using the same hardware is technically impossible. This is while the implemented setup includes a modern real-time embedded controller with 3 millions gates (CompactRIO made by National Instruments). It seems that the realization of ANC systems for controlling the noise propagating in free space is still a challenge. The main motivation for this research paper is dealing with this challenge.

II. ANC ROOT LOCUS ANALYSIS AND DESIGN

Bjarnason derived the following model for the dynamics of $w(n)$ in the FxLMS algorithm [2].

$$1 + \mu \sigma_x^2 \frac{s_m^2 z^m + s_{m+1}^2 z^{M-m-1} + \dots + s_M^2}{z^{M-1} (z-1)} = 0 \quad (2)$$

where σ_x^2 is the power of $x(n)$, M is the order of S and s_q denotes impulse response coefficients of S . In general, m can be equal to zero; but it should be greater than zero in practice because S implicates a propagation time delay. This model considers a general secondary path but Bjarnason had to simplify it by considering an ideal pure delay secondary path, when intending to obtain analytical results from it. Recently, we performed a root locus analysis on the model given in Eq. (2) considering a general secondary path [8], [10]. This analysis can apply to a realistic case with a general secondary path, unlike Bjarnason's analysis. Also, we determined some typical properties for the M branches of the FxLMS root locus (B_1, B_2, \dots, B_M) in [8]:

- 1) B_1 starts at $z = 1$ and moves towards the origin on the real axis.
- 2) B_2 starts at $z = 0$ and moves towards the unit circle on the positive real axis.
- 3) B_3, B_4, \dots and B_M start at $z = 0$ with different departure angles and move towards the unit circle.

These typical trajectories are shown in Fig. 2. As seen, B_1 and B_2 meet each other on the real-axis at a breakaway point

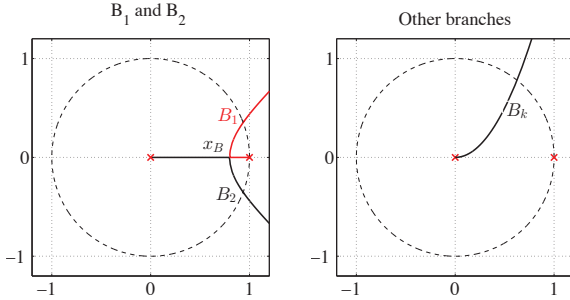


Fig. 2: Typical properties of the FxLMS root locus

x_B and then they leave the real-axis, moving towards the unit circle again. The location of x_B is given by [8]

$$x_B = D_{eq} (D_{eq} + 1)^{-1} \quad (3)$$

where D_{eq} is the secondary path equivalent delay defined as

$$D_{eq} = \frac{m s_m^2 + (m+1) s_{m+1}^2 + \dots + M s_M^2}{s_m^2 + s_{m+1}^2 + \dots + s_M^2} \quad (4)$$

As seen in Fig. 2, only B_1 starts at $z = 1$ and the other branches start at the origin. This means that for small values of μ , the root moving on B_1 is closer to the unit circle than the other roots. This behavior can be clearly seen in Fig. 2. As a conclusion, the dominant pole of the FxLMS root locus is located on B_1 . An example of the FxLMS root locus with a particular secondary path is given in Fig. 3a.

For the acoustic noise propagating in free space, D_{eq} is a large number because of the propagation delay implicated in S . In this case, one can conclude from Eq. (3) that x_B must be located close to the critical point ($z = 1$); consequently, the dominant root of the FxLMS root locus is located very close to the critical point, resulting in the high sensitivity of the adaptation process. This theoretical finding supports our practical observation that the FxLMS algorithm is very sensitive when it is used for controlling noise in free space. For developing a more robust update equation, we propose to modify the FxLMS update equation as:

$$\mathbf{w}(n+1) = a(n) \otimes \mathbf{w}(n) + \mu e(n) s(n) \otimes x(n) \quad (5)$$

where $a(n)$ denotes a linear filter impulse response. The logic behind choosing this structure for the proposed update equation is that it can introduce particular poles and zeros to the FxLMS root locus, without changing the original root locus structure. This issue can be seen later when comparing different root loci of the FxLMS algorithm and the proposed algorithm.

The update equation proposed in Eq. (5) is similar to the FxLMS update equation given in Eq. (1). However, in the proposed equation, $\mathbf{w}(n)$ is filtered by $a(n)$ before being updated. Using the same logic used in [8], the dynamic of the adaptation process performed by the proposed update equation can be modeled as

$$1 + \mu \sigma_x^2 \frac{s_m^2 z^m + s_{m+1}^2 z^{M-m-1} + \dots + s_M^2}{z^{M-1} (z - A(z))} = 0 \quad (6)$$

where $A(z)$ represents the transfer function of $a(n)$ in the z -domain. In [1], [10], we proposed a special case of Eq. (5), called the FwFxLMS (Filtered-W FxLMS) update equation. In the FwFxLMS update equation proposed in [1], [10], $A(z)$ has a simple recursive structure that introduces a single open-loop zero (ξ) to the FxLMS root locus. This zero causes the robustness of the FxLMS algorithm to be improved. For example, by setting $\xi = 0.5$, the FxLMS root locus shown in Fig. 3a changes to the root locus shown in Fig. 3b. As seen, the open-loop zero $\xi = 0.5$ causes that the trajectory of the dominant pole (B_1) does not return towards the unit circle, resulting in the robustness of the adaptation process. The adaptation process robustness is directly related to the distance of ξ to the origin: the smaller ξ , the more robust adaptation process. We verified this theoretical finding in an acoustic duct [1], [10]. We found that when the original FxLMS algorithm is used for active noise control in a duct, a sudden change in the acoustic plant causes the adaptation process to become unstable (high sensitivity); however, setting ξ into a proper location can stabilize the adaptation process and make it more robust [1].

When using the experimental setup in free space, we found that the robustness caused by this method is not sufficient and the process becomes unstable even without occurring any sudden change in the acoustic plant. This is mainly because, the FwFxLMS update equation given in [1], [10] is only more robust than the FxLMS update equation when ξ is higher than a lower-bound (ξ_{min}). The existence of this lower-bound restricts the achievable robustness level. For example, when $\xi = 0.4$ in the previous example, the adaptation process becomes even more sensitive than the original process. This is because ξ is set below $\xi_{min} = 0.45$. The root locus of this example is shown in Fig. 3c. As seen, the open loop located at $\xi = 0.4$ attracts other branches than B_1 ; therefore, B_1 (which is the branch containing the dominant pole) has to follow the typical trajectory shown in Fig. 2. In this case, B_1 moves toward the unit circle after reaching x_B , resulting in the adaptation process sensitivity. To remove this restriction, this paper proposes the following filter to be used in the FwFxLMS update equation.

$$A(z) = \frac{1 - 2\xi + (\xi^2 + \omega^2) z^{-1}}{1 - 2\xi z^{-1} + (\xi^2 + \omega^2) z^{-2}} \quad (7)$$

There are two criteria for choosing this form for $A(z)$. The first criterion is that the steady state gain of $A(z)$ should be 1 ($A_{ss}=1$) so that it does not affect the adaptation process steady state performance. Setting $z=1$ in Eq. (7) results in $A_{ss}=A(1)=1$; thus, the proposed structure meets the first criterion. The second criterion is that substituting $A(z)$ into Eq. (6) should result in the creation of the desired open-loop zeros or poles. Here, it is desired to create two complex conjugate open-loop zeros inside the unit-circle at $z_{1,2}=\xi \pm j\omega$. Substituting the proposed form of $A(z)$ into Eq. (6) results in the appearance of $z - z_1$ and $z - z_2$ factors in the nominator of the second term in Eq. (6). Thus, the proposed structure can also meet the second criterion.

When ξ and ω are set properly, the trajectory of B_1 can be pushed towards the origin, resulting in a more robust

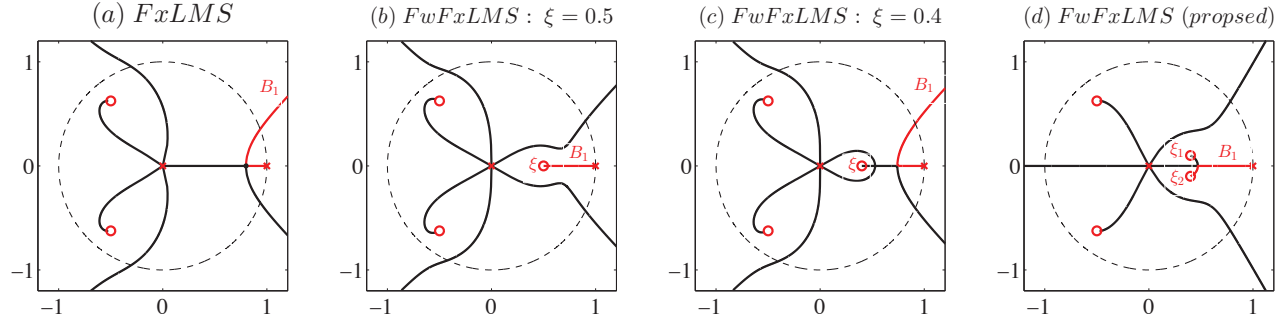


Fig. 3: FxLMS and FwFxLMS root loci for different cases

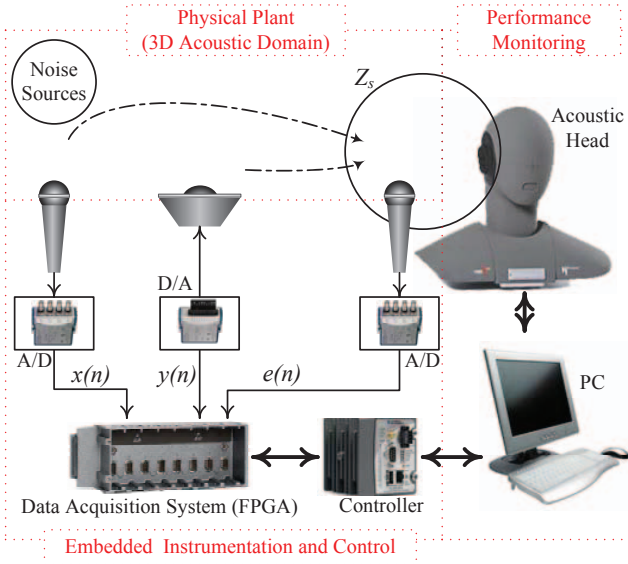


Fig. 4: A general scheme for embedded realization of single-channel feed-forward ANC

adaptation process. The robustness level achieved here is more than the robustness level achieved by the FwFxLMS algorithm proposed previously in [1], [10]. For the example discussed above, by setting $\xi=0.4$ and $\omega=0.1$, the root locus is changed to the one shown in Fig. 3d. As seen, even for $\xi=0.4$, B_1 does not move toward the unit circle once reaching the breakaway point. This is while setting $\xi=0.4$ in the previously proposed algorithm does not improve robustness of the adaptation process. This means that the the proposed update equation is more robust than the FxLMS and the previously-proposed FwFxLMS update equations. This issue can be seen by comparing root loci of Fig. 3.

In terms of computational complexity, the proposed update equation is comparable with that of the FxLMS update equation. The difference between the computational complexity of these two equations is only 4 addition and 3 multiplication operations.

III. EMBEDDED IMPLEMENTATION AND EXPERIMENTAL RESULTS

Fig. 4 shows a general scheme for the embedded implementation of single-channel feed-forward ANC. The microphone

located close to the noise source is called the reference microphone and the one located in Z_s is called the error microphone. The outputs of these microphones are fed to A/D modules to produce $x(n)$ and $e(n)$. The A/D modules are connected to a FPGA chassis, where signal acquisition and conditioning algorithms can be performed on the measured signals. This combination forms an embedded instrumentation system. Also, the FPGA chassis produces $y(n)$ which is then fed to a D/A module connected to the FPGA chassis. The output of the D/A module is then fed to a loudspeaker. The acoustic signal produced by the loudspeaker propagates through the medium to reach Z_s . Another hardware component of the proposed scheme is a real-time controller which configures the FPGA chassis. Also, this controller is responsible for transferring data between the FPGA chassis and a PC, where FPGA codes are compiled and the measured data are monitored, analyzed and recorded. The effects of the microphones, loudspeaker and other electro-acoustical components can be included in the primary and secondary paths [1]. In this case, the scheme, shown in Fig. 4, completely matches the model given in Fig. 1.

We implemented this scheme in a large anechoic room, where sound propagates in three spatial dimensions without any reflections (similar to free space). This setup includes a BEQ acoustic head which has a hearing system similar to the human hearing system. This acoustic head does not contribute to ANC operations; but it is used for monitoring the ANC system performance. This efficient and flexible experimental setup can be used for the embedded implementation of different ANC algorithms. Fig. 5 shows a photography of this setup. The loudspeaker used as the primary source produces a white noise. The error microphone is located very close to the right ear of the acoustic head and the signal heard by the acoustic head is recorded as a measure for evaluating the ANC system performance.

In the first experiment with this setup, the FxLMS update equation is implemented in the FPGA chassis. After activating the ANC system, the adaptation process starts at a very low convergence rate and, shortly after, it becomes unstable, as shown in Fig. 6a. In the second experiment, the FwFxLMS update equation, proposed previously in [1], [10], is implemented in the FPGA chassis. The result shows that the adaptation starts converging; however, the process becomes unstable after 0.015 seconds, as shown in Fig. 6b.

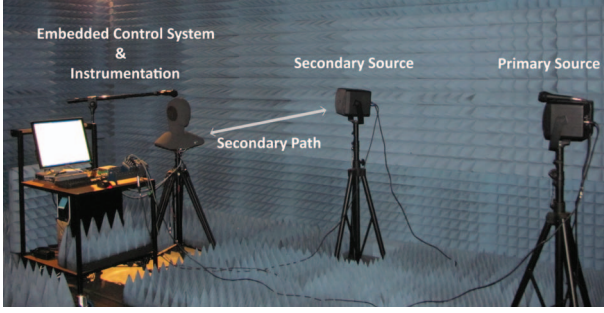


Fig. 5: Photography of the experimental setup

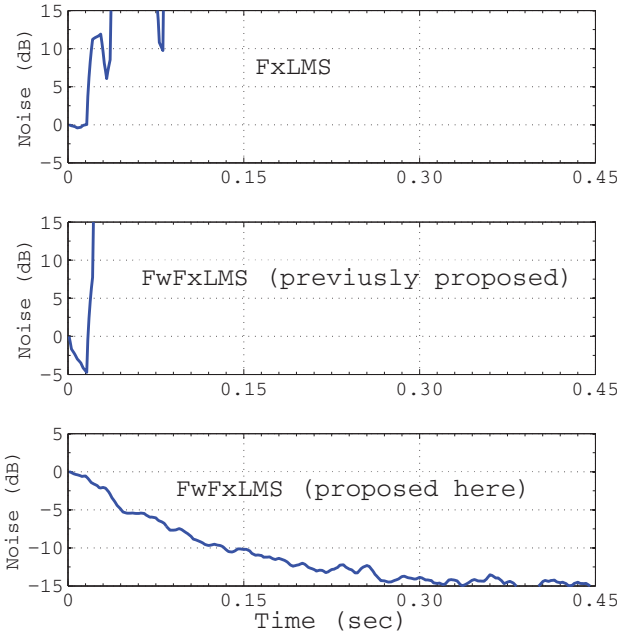


Fig. 6: Experimental results

In the third experiment the FwFxLMS update equation, as proposed in this paper, is implemented in the FPGA chassis. In this case, the adaptation process begins at a relatively high convergence rate and keeps its convergence behavior until the noise is reduced by 15 dB in steady state conditions. The above experiments can successfully be conducted for different geometrical arrangement of the ANC system components in the anechoic room.

IV. CONCLUSION

The FxLMS algorithm is an efficient ANC algorithm; however, this algorithm is only efficient for simple acoustic plants, e.g. acoustic ducts or headphones in practice. When this algorithm is used for active control of the noise propagating in three-dimensional free space, it shows insufficient robustness against changes in the characteristics of the noise or geometry of the acoustic plant. To solve this problem, an alternative update equation, proposed in this paper, is used. This update equation is derived through performing a root locus analysis on the dynamics of the FxLMS adaptation process. Using this

analysis, it is proved that the robustness of the adaptation process performed by the proposed update equation is higher than the robustness of the FxLMS adaptation process. Moreover, the computational complexity of the proposed update equation is comparable with the FxLMS update equation. This algorithm is found very efficient in practice as it can successfully attenuate the noise propagating in free space by about 15 dB.

V. ACKNOWLEDGMENT

This research is supported by The University of Auckland FRDF grant; Project Number: 3700501.

REFERENCES

- [1] Iman Tabatabaei Ardekani and Waleed H. Abdulla. Filtered weight fxlms adaptation algorithm: Analysis, design and implementation. *International Journal of Adaptive Control and Signal Processing*, 25(11):1023–1037, 2011.
- [2] E. Bjarnason. Analysis of the filtered-x LMS algorithm. *IEEE Transactions on Speech and Audio Processing*, 3(6):504–514, Nov. 1995.
- [3] J. C. Burgess. Active adaptive sound control in a duct: computer simulation. *Journal of the Acoustical Society of America*, 70:715–726, 1981.
- [4] S. J. Elliott. *Signal Processing for Active Control*. Academic Press, San Diego, CA., 2001.
- [5] W.S. Gan and S.M. Kuo. An integrated audio and active noise control headset. *IEEE Transactions on Consumer Electronics*, 48(2):242–247, May 2002.
- [6] W.S. Gan, S. Mitra, and S.M. Kuo. Adaptive feedback active noise control headset: implementation, evaluation and its extensions. *IEEE Transactions on Consumer Electronics*, 51(3):975–982, Aug. 2005.
- [7] I. Tabatabaei Ardekani and W.H. Abdulla. On the convergence of real-time active noise control systems. *Signal Processing*, 91(5):1262 – 1274, 2011.
- [8] I. Tabatabaei Ardekani and W.H. Abdulla. On the stability of adaptation process in active noise control systems. *Journal of Acoustical Society of America*, 129(1):173–184, 2011.
- [9] I. Tabatabaei Ardekani and W.H. Abdulla. Effects of imperfect secondary path modeling on adaptive active noise control systems. *Control Systems Technology, IEEE Transactions on*, 20(5):1252 –1262, sept. 2012.
- [10] I. Tabatabaei Ardekani and W.H. Abdulla. Root locus analysis and design of the adaptation process in active noise control. *Journal of Acoustical Society of America*, 132(4):2313–2325, 2012.
- [11] Yoshinobu Kajikawa, Woon-Seng Gan, and Sen M. Kuo. Recent advances on active noise control: open issues and innovative applications. *APSIPA Transactions on Signal and Information Processing*, 1, 2012.
- [12] S. M. Kuo and D. R. Morgan. *Active noise control systems: algorithms and DSP implementations*. Wiley Interscience, New York, NY, USA, 1996.
- [13] S.M. Kuo, S. Mitra, and Woon-Seng Gan. Active noise control system for headphone applications. *IEEE Transactions on Control Systems Technology*, 14(2):331–335, Mar. 2006.
- [14] R.M. Reddy, I.M.S. Panahi, R. Briggs, and E. Perez. Performance comparison of fxrls, fxapa and fxlms active noise cancellation algorithms on an fmri bore test-bed. In *Engineering in Medicine and Biology Workshop, 2007 IEEE Dallas*, pages 130 –133, nov. 2007.
- [15] B. Widrow, D. Shur, and S. Shaffer. On adaptive inverse control. In *Proceeding of the 15th Asilomar Conference on Circuits, Systems and Computers*, pages 185–189, Nov. 1981.
- [16] Ya-Li Zhou, Qi-Zhi Zhang, Xiao-Dong Li, and Woon-Seng Gan. On the use of an SPSA-based model-free feedback controller in active noise control for periodic disturbances in a duct. *Journal of Sound and Vibration*, 317(3):456 – 472, 2008.